

# Linewidths and shifts of very low temperature CO in He: A challenge for theory or experiment?

Mark Thachuk

*Department of Chemistry, Queen's University, Kingston, Ontario K7L 3N6, Canada*

Claudio E. Chuaqui

*Department of Chemistry, University of British Columbia, 2036 Main Mall, Vancouver, British Columbia V6T 1Z1, Canada*

Robert J. Le Roy

*Guelph-Waterloo Center for Graduate Work in Chemistry, University of Waterloo, Waterloo, Ontario N2L 3G1, Canada*

(Received 15 April 1996; accepted 31 May 1996)

The pressure broadening and shifting coefficients for pure rotational transitions of CO in a He bath gas at very low temperatures are calculated from the best available potential energy surfaces, and compared with very recent measurements by M. M. Beaky, T. M. Goyette, and F. C. De Lucia [J. Chem. Phys. **105**, 3994 (1996)]. The results obtained for two recent empirical potentials determined from fits to Van der Waals spectra, and for a recent high quality purely *ab initio* surface, are consistent with one another. The best of the spectroscopic potentials also yields good agreement with high temperature virial coefficients and transport properties. Predictions from all three of these potentials agree with linebroadening and shifting measurements at temperatures above  $\sim 20$  K, but are in substantial disagreement with the measurements at temperatures below 4 K. At present, the source of this discrepancy is not known. © 1996 American Institute of Physics. [S0021-9606(96)00934-8]

## I. INTRODUCTION

In recent years, the broadening and shifting of pure rotational transitions of CO by collisions with He has attracted considerable experimental and theoretical attention.<sup>1-9</sup> Interest in this system arose partly because of the practical importance of its low temperature inelastic cross sections in interpreting astronomical data, and partly because it has become a popular test case regarding our ability to determine accurate anisotropic potential energy surfaces for heavy (i.e., nonhydride) rotor systems. In the latter regard, puzzling questions have recently been raised by apparent contradictory conclusions regarding the nature of the potential energy surface for He-CO. In particular, the long-accepted *ab initio* He-CO surface of Thomas, Kraemer, and Dierksen<sup>9</sup> completely fails to account for the observed discrete infrared spectra of the Van der Waals dimers,<sup>8</sup> but yields predictions in partial agreement with low temperature CO line broadening cross sections.<sup>3,6,8</sup> In contrast, potentials which accurately represent the discrete infrared spectra of the Van der Waals molecule seriously overestimate the published experimental line broadening cross sections.<sup>8</sup>

Conventional wisdom would tend to blame such discrepancies on inadequacies of the potential energy surfaces used. In particular, since the very low temperature line broadening measurements and the Van der Waals spectra are both dilute-gas properties primarily sensitive to the interaction minima, it seems reasonable to expect that a "true" Born-Oppenheimer potential surface for the He-CO system must account for both phenomena. It might, therefore, be natural to conclude that none of the surfaces investigated provides a realistic approximation to the true interaction, and that some

other surface could be devised which is able to model all of the experimental data.

The above argument presumes that the experimental observables in question can be calculated unambiguously from a given potential surface. Without a reliable and accurate connection between a potential surface and a given observable, it is not meaningful to use those experimental data as a test for the surface, nor is it possible to extract information about the interaction from the measurements. Simulation of the discrete infrared spectra involves calculation of the properties of individual quantum states lying in the potential well, without any of the layers of averaging associated with scattering or bulk property measurements. The calculation of the requisite level energies and wave functions in turn requires the solution of the full Schrödinger equation for nuclear motion of the system. However, the bound rotation-vibration energy levels and wave functions of most atom-diatom systems can be determined essentially "exactly" (or to arbitrary precision) by any of a number of methods,<sup>10-17</sup> without the need to impose simplifying approximations. Thus, the simulation of the infrared data is not the source of the problem.

The situation is less clear for the calculation of spectral line shape parameters, especially at cryogenic temperatures. For the case of an electric-dipole spectrum in the weak radiation field limit, the spectral line shape is related to the Fourier transform of the (bulk gas) system dipole moment function. This is a many-body problem involving all of the species in the bulk, and it is necessary to impose a hierarchy of approximations in order to render the line shape calculation tractable (see, e.g., the review by Green<sup>18</sup>). First, the many-body problem is simplified to the case of a process

involving a single chromophore species in a bath of perturbing molecules. To arrive at the Shafer–Gordon<sup>19</sup> formalism used to obtain pressure broadening cross sections, the problem is further reduced to one involving only binary collisions between the absorber and a single perturber, thus allowing the use of computationally accessible binary collision  $S$  matrix elements. This second step is accomplished by invoking the impact approximation,<sup>19</sup> which assumes that collisions are short in duration when compared to the time between collisions. Note, however, that the approximations introduced in this procedure are in the kinetic theory part of the derivation, and not in the scattering calculations, which are essentially exact.

In view of this situation, Ref. 8 proposed that the discrepancy regarding the potentials required to explain the line broadening and the discrete infrared spectra may actually be due to a breakdown of conventional line broadening theory at the very low temperatures (1.7–4.4 K) associated with the available line broadening measurements.<sup>3,4</sup> In an effort to resolve this question, Sec. II summarizes the properties of a number of the recently proposed potentials for this systems, and critically compares their abilities to explain a variety of experimental data. Section III then reports extensive line broadening and shifting calculations performed for four of these potential energy surfaces, and compares their predictions with new very low temperature measurements of Beaky *et al.*<sup>20</sup> These results are then discussed and our conclusions presented in Sec. IV.

## II. POTENTIAL ENERGY SURFACES FOR He–CO

### A. Recently proposed surfaces

Over the years, interest in the He–CO system has motivated numerous efforts to predict or determine its anisotropic potential energy surface. Early calculations of its collisional properties were based on relatively simplistic model potentials,<sup>18,21</sup> but in 1980 Thomas, Kraemer, and Dierksen<sup>9</sup> used *ab initio* self-consistent-field configuration interaction methods to calculate the “TKD” potential,  $V_{\text{TKD}}$ , which is regarded as the first semiquantitative theoretical potential surface for this system. At the time, the main experimental property against which the existing potentials could be tested were the pressure broadening cross sections for the pure rotational transitions of CO perturbed by He, measured at temperatures between 77 and 300 K.<sup>5</sup> However, those data were unable to distinguish between the existing surfaces, and it was not until advances in experimental techniques permitted the measurement of linewidths for the  $R(0)$ ,  $R(1)$ , and  $R(2)$  transitions of CO at cryogenic temperatures<sup>3,4</sup> that the  $V_{\text{TKD}}$  surface was found to be superior to the older surfaces, and in reasonable agreement with those experiments.<sup>6,7,18</sup>

Since the linewidth measurements at cryogenic temperatures had been shown to be particularly sensitive to the well region of the potential,<sup>7</sup> this agreement with the line broadening measurements led to the general conclusion that the TKD potential provided a reasonably accurate description of the interaction between He and CO in the potential well and low energy repulsive wall regions. As a result, efforts to

explain certain other experimental properties of this system have been based on making small adjustments to portions of the TKD surface. In particular, Dilling showed<sup>22</sup> that elastic and inelastic differential scattering cross sections would be well reproduced if the first three Legendre radial strength functions of the potential expansion

$$V_{\text{TKD}}(r, \theta) = \sum_{\lambda=0} V_{\lambda}(r) P_{\lambda}(\cos \theta) \quad (1)$$

were shifted to larger distances by 1.0%, 1.0%, and 1.5%, respectively (here,  $r$  is the distance from the CO center of mass to the He atom and  $\theta$  the angle between that axis and the CO bond, with  $\theta=0$  corresponding to the collinear alignment O–C–He). More recently, Gianturco *et al.*<sup>23</sup> showed that equivalent agreement with the scattering data and better agreement with various transport properties could be obtained if the isotropic ( $\lambda=0$ ) part of  $V_{\text{TKD}}$  was shifted 0.75% to *smaller* distances and the remaining radial strength functions left unchanged. In both of these modified surfaces, however, the strength scaling parameters of the various anisotropy strength functions were unchanged, and recent analyses of the discrete infrared spectra of the weakly bound He–CO dimers shows that the associated potential well behavior is substantially incorrect.<sup>8,24</sup>

In recent years knowledge about intermolecular forces has been extracted from a diverse set of experimental measurements, including spectroscopic data, elastic and inelastic scattering cross sections, nonideal gas behavior, and a variety of bulk gas transport properties.<sup>25</sup> Of these properties, the discrete infrared spectra for weakly bound Van der Waals complexes are generally accepted as the best single source of information regarding the anisotropic potential energy wells of atom–molecule dimers.<sup>8,10,26–29</sup> In particular, data of this type have recently been used to determine two independent (but very similar) model potentials for the He–CO system. When those spectra were first obtained for He–CO, conventional spectroscopic methods were unable to assign most of the observed lines, and predictions based on the TKD potential completely failed to reproduce even the qualitative features of the observed spectra.<sup>8</sup> Moreover, it was demonstrated that the inability of  $V_{\text{TKD}}$  to account for the spectra was largely due to its underestimation of the potential well depth and its anisotropy,<sup>8</sup> precisely those features of the surface believed to be important for the broadening cross sections at cryogenic temperatures.

Careful analysis of synthetic spectra predicted from plausible realistic model potentials eventually yielded unique assignments for all of the observed discrete infrared transitions, and led to the determination of the semiempirical  $V_{333}$  potential energy surface for He–CO.<sup>8</sup> In subsequent work, a completely different potential form based on an exchange-Coulomb model, was determined from a fit of equal quality to the same set of infrared transitions, leading to the “XC(fit)” model potential,  $V_{\text{XC}}$ .<sup>24</sup> Although, the theoretical basis, type of model function, and parametrization were very different from those for the  $V_{333}$  potential, the final fitted  $V_{\text{XC}}$  surface has essentially equivalent behavior in the well re-

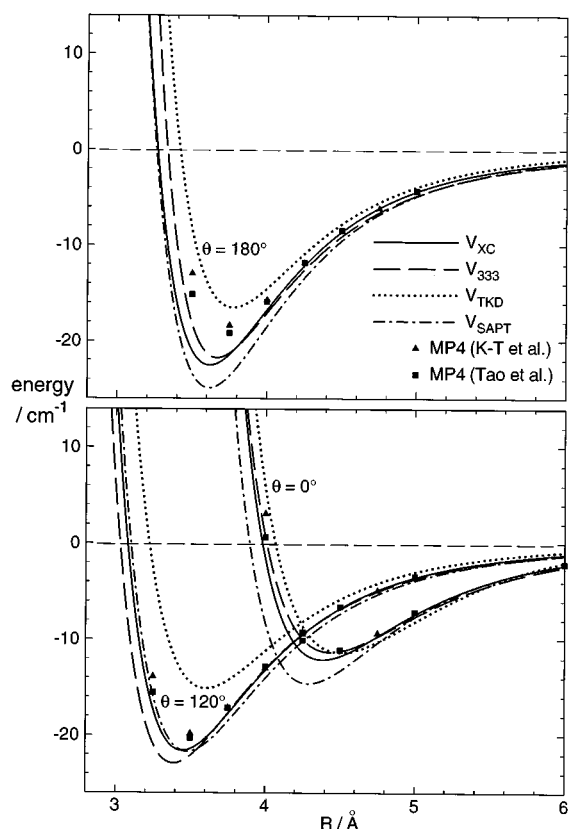


FIG. 1. Radial cuts through various proposed potential energy surfaces (see the text) for He-CO.

gion. In other words, the discrete Van der Waals spectra require the potential surface to have a very narrowly specified potential well depth, position and shape in the well region, *irrespective* of the functional form used to represent the interaction.

In the past couple of years, substantially improved *ab initio* potentials have also been reported for the He-CO system. In particular, both Kukawska-Tarnawska *et al.*<sup>30</sup> and Tao *et al.*<sup>31</sup> reported calculations based on fourth-order Moeller-Plesser perturbation theory (MP4), while Moszynski *et al.*<sup>32</sup> obtained a full two-dimensional surface using the symmetry-adapted perturbation theory (SAPT) approach. The properties of the wells of these new theoretical surfaces are in good qualitative agreement with those of the spectroscopy-based  $V_{333}$  and  $V_{XC}$  potentials. However, Kukawska-Tarnawska *et al.*<sup>30</sup> did not report an analytic form for their surface, so we chose to focus our attention on the SAPT potential of Moszynski *et al.*<sup>32</sup>

## B. Critical comparisons of the recently proposed surfaces

Figure 1 compares cuts through the attractive wells of the various potential energy surfaces considered for this system. The similarity of the solid ( $V_{XC}$ ) and long-dash ( $V_{333}$ ) curves demonstrates the essentially equivalent nature of the

well regions of these two spectroscopic potentials. At the same time, since these two surfaces yield equally good representations of the discrete infrared data on which they are based (with average line position discrepancies of less than  $0.002 \text{ cm}^{-1}$ ), the differences between them provides a quantitative indication of the effect of model dependence in that analysis. In the repulsive wall region more substantial differences may be expected (see Fig. 3 of Ref. 24), since the empirical form of the  $V_{333}$  function means that its behavior there is based on a blind extrapolation from the (fitted) well region, while the theoretical basis of the XC(fit) potential form leads us to expect that its extrapolation behavior should be quite realistic. This expectation is confirmed by the comparisons for higher temperature ( $T=123\text{--}473 \text{ K}$ ) bulk properties reported by Dham and Meath<sup>33</sup> (see below).

The dotted curves in Fig. 1 show that the original TKD potential<sup>9</sup> is distinctly shallower and has a much smaller well-depth anisotropy than the two empirical spectroscopic surfaces. Overall, the attractive well of  $V_{TKD}$  lies at larger intermolecular distances, and for the deeper cuts, its zero potential crossing points (the distance known as “ $\sigma$ ”) lie at distances 3%–5% larger than those for  $V_{XC}$  or  $V_{333}$ . Relative to these large differences, the modified TKD-type potentials of Dilling<sup>22</sup> and Gianturco *et al.*<sup>23</sup> (displaced in  $r$  by between +1.0 and 1.5%, and by  $-0.75\%$ , respectively) may be considered essentially equivalent to  $V_{TKD}$  in the well region. The inadequacy of the potential wells of these three TKD-based potentials is manifested by the fact that  $V_{TKD}$  supports only a fraction of the bound levels seen experimentally, and that its simulated infrared spectrum shows little similarity with the experimental one.<sup>8</sup> Thus, the discrete infrared data clearly demonstrate that the potential well properties of  $V_{TKD}$  and the variants proposed by Dilling<sup>22</sup> and Gianturco *et al.*<sup>23</sup> are substantially incorrect.

Figure 1 also shows that the attractive wells of the *ab initio* SAPT and MP4 potentials are fairly similar to those of the  $V_{XC}$  and  $V_{333}$  surfaces, and calculations reported by Moszynski *et al.*<sup>32</sup> (see their Figs. 6–8) demonstrated that the infrared spectrum of the SAPT surface is fairly similar to experiment. At the same time, the root mean square discrepancy between experiment and the predicted infrared line positions for the SAPT surface ( $\sim 0.2 \text{ cm}^{-1}$ ) is more than 100 times larger than the values for the empirical XC and  $V_{333}$  potentials. Thus, the qualitative similarity of these *ab initio* potentials with the  $V_{XC}$  and  $V_{333}$  functions provides independent confirmation of the essential validity of the latter, but the two empirical surfaces are unquestionably more accurate in the well region.

The discrete infrared spectra clearly depend on the properties of individual quantum states lying in the potential well, and hence may be thought of as a definitive “low temperature” property of the system. In contrast, Dham and Meath<sup>33</sup> have tested a number of the proposed surfaces against experimental values of “high temperature” bulk properties, which depend mainly on the position and anisotropy of the short-range repulsive wall. Those results, summarized in Table I, clearly indicate that although their potential wells are equivalent (at least as far as the infrared data are con-

TABLE I. Root-mean-square % deviations from experiment of bulk properties calculated from four proposed potentials for He–CO (results from Ref. 33).

Property	Temperature range (K)	Potential			
		XC (fit)	$V_{333}$	TKD	Gianturco <i>et al.</i>
Interaction second virial coefficients	123–273	2.8	3.0	35.0	26.0
Binary diffusion coefficients	277–473	0.90	3.96	1.10	1.25
Interaction viscosity coefficients	298–473	0.82	2.69	3.30	1.08
Mixture viscosity coefficients	298–473	0.32	1.07	1.32	0.42

cerned), the XC surface has a distinctly more realistic repulsive wall than does the  $V_{333}$  function. Moreover, both spectroscopic potentials yield far better agreement with the experimental second virial coefficients, especially at the lower temperatures,<sup>33</sup> and the XC potential's predictions of the transport properties are also significantly better than those of both the original TKD potential<sup>9</sup> and Gianturco *et al.* modified version of that function.<sup>23</sup> Thus, all of these properties seem to agree on the overall superiority of the XC(fit) surface.

One further test for these potential energy surfaces is provided by the measured total and inelastic differential cross sections for this system.<sup>34,35</sup> Improving the agreement with these data was the motivation for Dilling's modification of the TKD potential,<sup>22</sup> and was used to support the adjustment (in the opposite direction) proposed by Gianturco *et al.*<sup>23</sup> Unfortunately, neither the raw experimental data nor a prescription for performing the experimental apparatus averaging have appeared in the open literature. However, a useful comparison of these potentials may still be obtained by comparing the calculated centre of mass cross sections with each other.

For the XC(fit) potential and both the Dilling and Gianturco *et al.* modifications of the TKD surface, differential cross sections at the experimental collision energy of 27.7 meV ( $223 \text{ cm}^{-1}$ ) were calculated using essentially exact close-coupling calculations. The computations were performed with the Hutson–Green MOLSCAT program<sup>36</sup> using the Manolopoulos propagator<sup>37</sup> with an integration mesh defined by setting parameter STEPS=20 and an integration range which extended to RMAX=30 Å. The angular basis included all of the 11 channels open at this collision energy, as well as the first two closed channels (for  $j=11$  and 12), and the partial wave sum went up to  $J_{\text{TOT}}=80$ ; the requisite channel energies were defined by the molecular constants of Varberg and Evenson.<sup>38</sup> The angular expansion for the two TKD-based potentials included all of its seven terms, while that for the XC(fit) potential was performed using (numerically determined) radial strength functions for Legendre terms up to  $\lambda=10$ . Tests indicated that these calculations yielded integral elastic and inelastic cross sections converged to better than 0.04%. The  $S$ -matrix elements yielded by MOLSCAT were then combined to yield differential cross sections using a program kindly provided by Sheldon Green. The total differential cross sections were obtained by adding elastic and inelastic differential cross sections for all (eleven) open channels, using the reported<sup>22</sup> initial-state population

weighting factors of 0.65, 0.27, 0.07, and 0.02 for  $j=0$  to 3, respectively.

The leading inelastic differential cross-sections obtained in the manner described above for the XC(fit) potential and the Dilling and Gianturco *et al.* modifications of the TKD surface are compared in Fig. 2. While there are modest differences, especially for  $j=0 \rightarrow 2$ , the dominant overall observation is that the results for the three potentials are remarkably similar. Allowing for the effect of further averaging over experimental conditions and apparatus parameters, it seems clear that these three surfaces provide essentially equivalent predictions of the inelastic differential cross sections. As might be expected, the three sets of  $\Delta j=1$  cross sections for  $j(\text{initial})=0-2$  are qualitatively quite similar to one another, with the overall magnitude decreasing as the energy gap grows with  $j(\text{initial})$ .<sup>39</sup>

Figure 3 presents analogous comparisons of the total differential cross sections predicted from these three surfaces. Once again, they are remarkably similar. This may seem somewhat surprising, since conventional wisdom argues that the positions and spacings of the interference oscillations in total cross sections are largely determined by the position and slope of the isotropic or spherically averaged potential at its zero crossing distance  $\sigma$ , and Fig. 4 shows that the modified TKD potentials are quite different than the XC(fit) function there. It is interesting to note, however, that the XC(fit) and Gianturco *et al.* functions are much more similar near the experimental collision energy of  $223 \text{ cm}^{-1}$ . In any case, allowing for the effect of averaging over the experimental conditions and for calibration errors in the angular measurements,<sup>40</sup> it again appears that the XC(fit) potential yields predictions essentially equivalent to the two modified TKD functions.

In conclusion, therefore, we see that the XC(fit) potential yields distinctly superior agreement with the discrete infrared transitions<sup>24</sup> and with high temperature bulk property measurements,<sup>33</sup> and is essentially equivalent to the modified TKD potentials of Dilling<sup>22</sup> and Gianturco *et al.*<sup>23</sup> with regard to the elastic and inelastic differential cross sections. It must therefore be recognized as the most accurate potential surface currently available for the He–CO system, especially in the potential well and low energy repulsive wall region expected to be of dominant importance for the very low temperature line broadening and shifting cross sections.

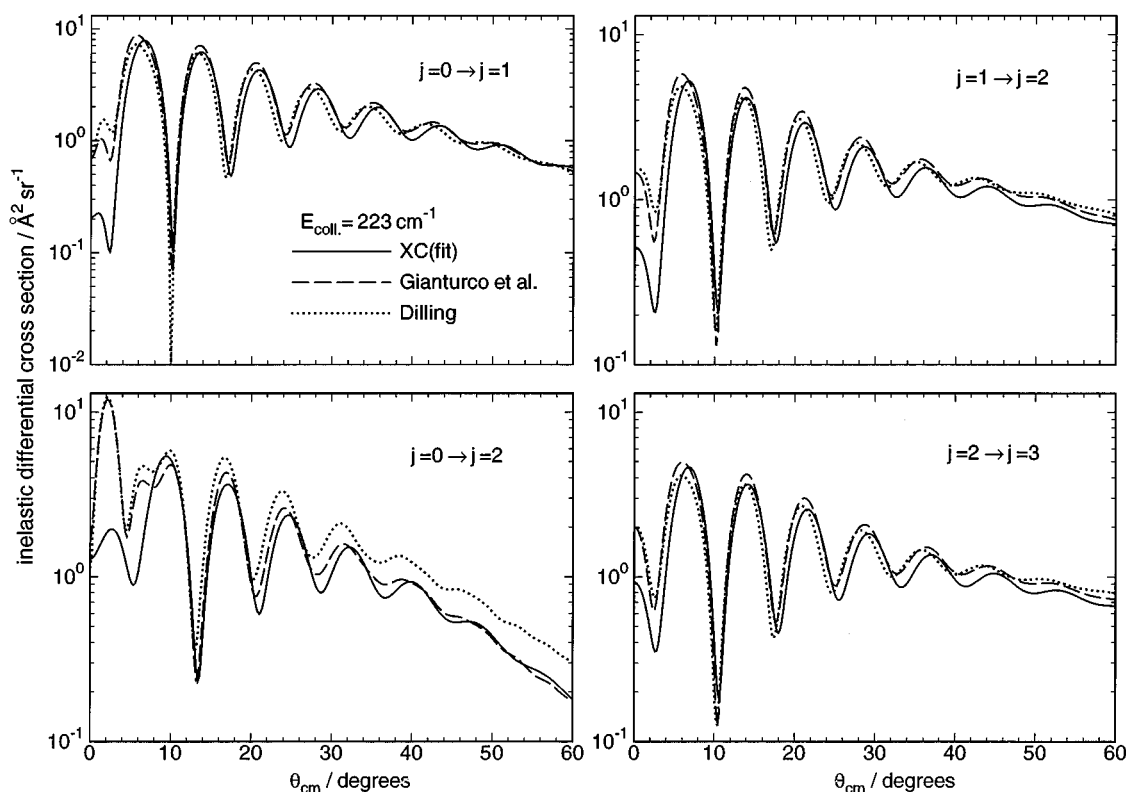


FIG. 2. Inelastic differential cross sections for He–CO predicted by close coupling calculations using the spectroscopy-based XC(fit) potential (Ref. 24) and the Dilling (Ref. 22) and Gianturco *et al.* (Ref. 23) modifications of the TKD (Ref. 9) potential.

### III. LINE BROADENING AND SHIFTING CALCULATIONS

#### A. Methodology

When a diatom diluted in a bath gas undergoes a spectral transition, the central frequency of the transition can be shifted relative to its value in the absence of the bath gas, and the half-width at half-maximum of the line shape can change. These effects are the result of collisions occurring

between the diatom and bath gas during the spectral transition. Using kinetic theory, it is possible to express the half-width,  $\Delta\omega_{1/2}$ , and the shift,  $\omega - \omega_0$ , for a  $j_\beta \leftarrow j_\alpha$  transition as<sup>19</sup>

$$\Delta\omega_{1/2} = n\bar{c}_r \operatorname{Re}[\sigma] \quad (2)$$

and

$$\omega - \omega_0 = -n\bar{c}_r \operatorname{Im}[\sigma], \quad (3)$$

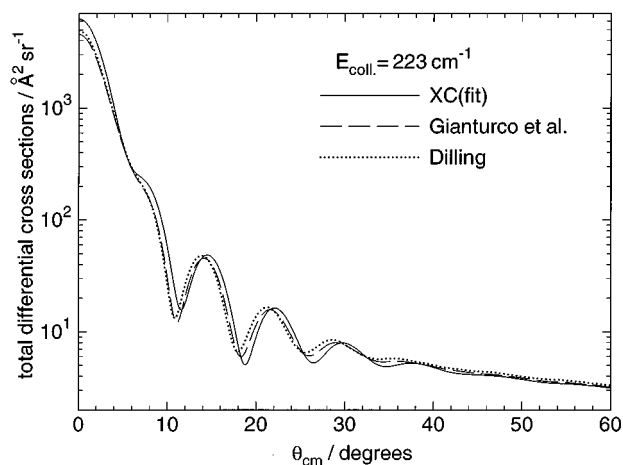


FIG. 3. Total differential cross sections for He–CO predicted by close coupling calculations, as in Fig. 2.

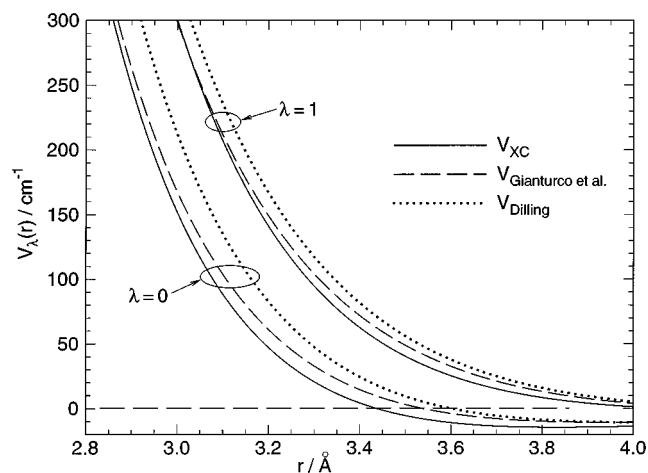


FIG. 4. Comparison of the isotropic and leading anisotropic radial strength functions [see Eq. (1)] for the three potentials considered in Figs. 2 and 3.

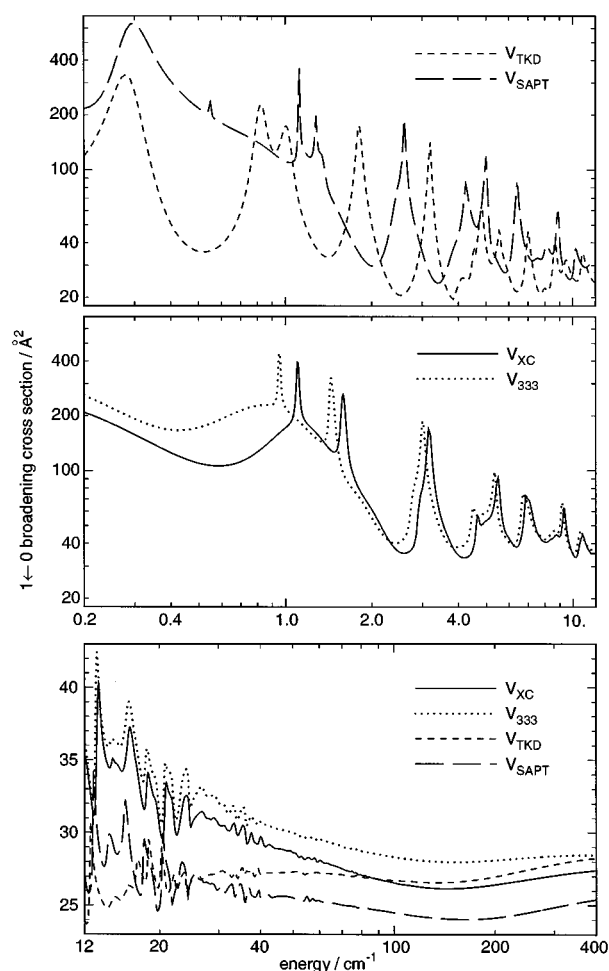


FIG. 5. Energy dependent  $j=1\leftarrow 0$  line broadening cross sections for He-CO, calculated using the empirical spectroscopic XC (fit) (Ref. 24) and  $V_{333}$  (Ref. 8) functions, and the *ab initio* TKD (Ref. 9) and SAPT (Ref. 32) potential energy surfaces.

where

$$\bar{c}_r = (8k_B T / \mu \pi)^{1/2} \quad (4)$$

is the average relative speed of the atom-diatom colliding pair,  $n$  is the number density of the bath gas,  $\mu$  the reduced mass of the atom-diatom pair,  $\sigma$  the broadening/shifting cross section for the transition of interest, and  $\omega_0$  is the spectral transition frequency of the diatom in the absence of a bath gas.

It should be noted, that in the full theoretical description of Shafer and Gordon,<sup>19</sup> the cross sections form a complex matrix whose diagonal elements are those used in Eqs. (2) and (3), and whose off-diagonal elements represent the transfer of intensity from one spectral transition to another. In the present work, the effect of the off-diagonal elements was examined by calculating the full cross-section matrix, and comparing the resulting shifts and widths with those predicted by using only the diagonal elements. The resulting values were indistinguishable, showing that the off-diagonal elements had negligible effect in this case. In calculating the results using the full description, it is necessary to specify a

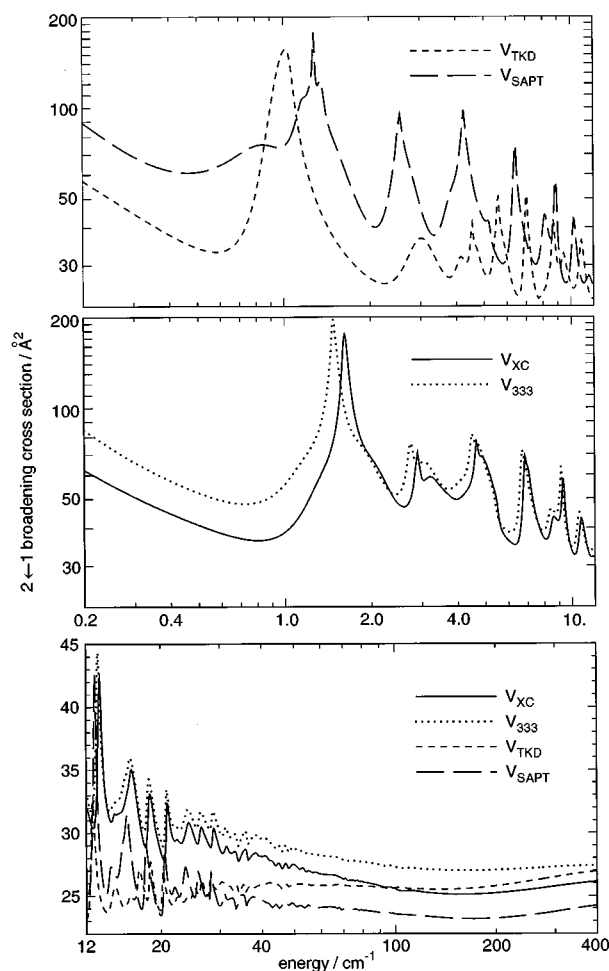


FIG. 6. For the  $j=2\leftarrow 1$  line broadening cross sections of He-CO, as in Fig. 5.

pressure at which the spectrum is desired; it was chosen here to be typical of that used in the experiments,<sup>3,4,20</sup> namely  $1 \times 10^{-3}$  Torr. At this pressure, the widths of the spectral lines are very narrow compared to the spacing between adjacent lines. This is the main reason that the off-diagonal elements, even though nonzero, have little effect on the final shifts and widths. At significantly higher pressures, the off-diagonal elements do contribute, and must be taken into account. However, that pressure regime is beyond the scope considered in this paper. Finally, the ideal gas law was used to determine the value of  $n$  appearing in Eqs. (2) and (3). This is justified because it can be shown that even at the lowest temperatures considered in the experiments, the behavior of the helium bath gas is very close to ideal.

The temperature dependent broadening/shifting cross sections appearing in Eqs. (2) and (3) are obtained by thermally averaging the corresponding kinetic energy dependent cross sections. These latter cross sections are generated from  $S$  matrix elements obtained from converged close-coupled calculations which describe the scattering event between the diatom and the atom. The details of the methods used in obtaining the various cross sections are given in Ref. 41. It should be noted, that the highest collision energy for which

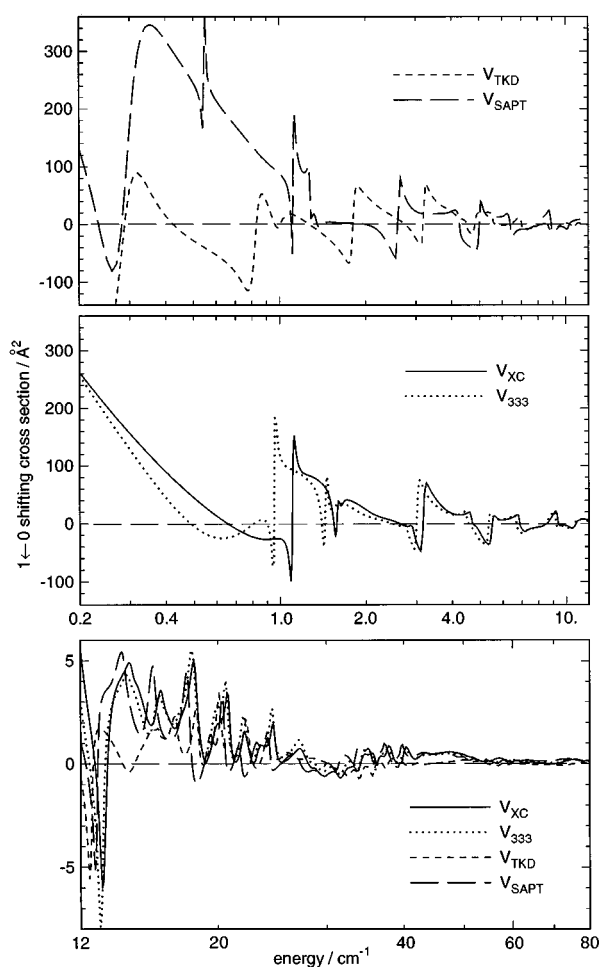


FIG. 7. For the  $j=1 \leftarrow 0$  line shifting cross sections of He-CO, as in Fig. 5.

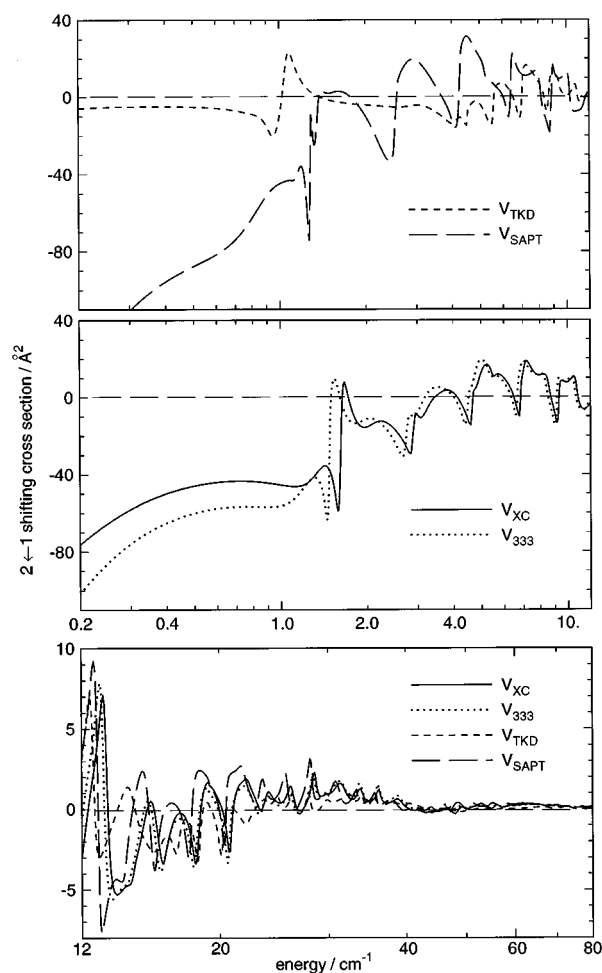


FIG. 8. For the  $j=2 \leftarrow 1$  line shifting cross sections of He-CO, as in Fig. 5.

cross sections were calculated ( $490 \text{ cm}^{-1}$ ) may seem quite modest when attempting to determine thermal cross sections for temperatures up to 300 K. Indeed, at the highest temperatures, energies up to this maximum account for only about half the contribution to some of the thermal averages. However, the behavior of the energy dependent cross sections was found to become *very* smooth near this maximum energy, so that accurate extrapolations can be made to higher energies. Use of a variety of different extrapolating schemes yielded high temperature cross sections which varied by less than 1%, and had essentially no effect on the results for  $T \leq 100 \text{ K}$ .

Close-coupled calculations of line broadening and shifting cross sections for the pure rotational  $j=0 \rightarrow 1$  and  $1 \rightarrow 2$  transitions of CO in helium were performed for the following four potential energy surfaces: the original TKD potential of Thomas *et al.*,<sup>9</sup> the empirical  $V_{333}$  and XC(fit) potentials determined from fits to the discrete infrared Van der Waals molecule spectra,<sup>8,24</sup> and the *ab initio* SAPT potential of Moszynski *et al.*<sup>32</sup> The requisite  $S$ -matrix elements were generated using the MOLSCAT program of Hutson and Green,<sup>36</sup> again employing the propagator of Manolopoulos.<sup>37</sup>

Very fine energy mesh calculations are required to fully resolve the detailed resonant structure in the kinetic energy dependent cross sections. This is crucial if reliable very low temperature spectral shifts and widths are to be obtained, since their values are completely dominated by the resonant structure. The energy grid employed is as follows: for the kinetic energy ranges 0.002–0.098, 0.1–1.99, 2.0–19.95, 20.0–29.9, 30.0–39.8, 40–99, and 100–200  $\text{cm}^{-1}$ , energy steps of 0.002, 0.01, 0.05, 0.1, 0.2, 1.0, and 10  $\text{cm}^{-1}$ , respectively, were used. A number of higher energy calculations at 240, 360, and 490  $\text{cm}^{-1}$  were also performed, in order to give fully converged higher temperature results. All closed channels which lay within 80  $\text{cm}^{-1}$  of the total energy were included in each calculation. The cutoffs in the total angular momentum summation ranged from  $J_{\text{TOT}}=5$  at the very lowest energies, to 50 at the highest energies, and convergence with respect to this cutoff was verified by examining the magnitudes of the terms in the sums over this total angular momentum for each cross section. As above, the rotational channel energies were taken from the results of Varberg and Evenson.<sup>38</sup>

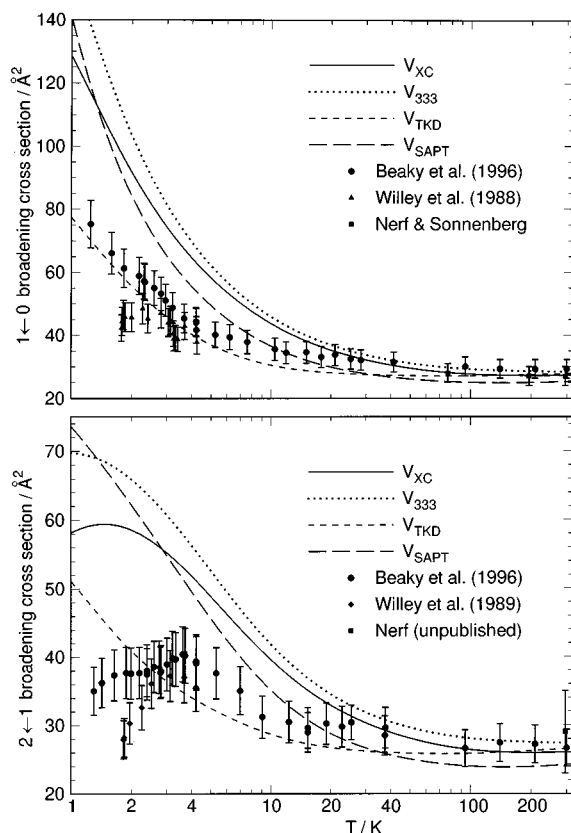


FIG. 9. Comparison with experiment (see the text) for thermal  $j=1\leftarrow 0$  and  $j=2\leftarrow 1$  line broadening cross sections of He-CO, calculated using the empirical spectroscopic XC(fit) (Ref. 24) and  $V_{333}$  potentials (Ref. 8), and the *ab initio* TKD (Ref. 9) and SAPT (Ref. 32) potential energy surfaces.

## B. Results

Figures 5–8 present the calculated pressure broadening and line shifting cross sections for the  $1\leftarrow 0$  and  $2\leftarrow 1$  pure rotational transitions of CO in He. In each case, the two upper panels span the low energy range using double logarithmic scales, while the bottom panel shows the high energy results with a linear scale being used for the cross sections. For all four properties, the magnitude and the resonance structure associated with cross sections for the two empirical spectroscopic potentials (e.g., middle panels) are quite similar. This is expected, since this structure is a manifestation of the energies and widths of quasibound level (tunneling predissociation) and Feshbach resonances, so potentials based on the discrete infrared spectra should be quite similar in this regard. In contrast, cross sections obtained for the TKD potential are markedly different, especially at low collision energies where their smaller magnitude can be attributed to the fact that its shallower well depth means that this potential supports fewer bound (and hence fewer metastable) levels.<sup>7</sup>

Performing the appropriate thermal averaging over these calculated cross sections then yields the thermal line broadening and shifting cross sections compared with experiment (points with error bars) in Figs. 9 and 10. All of the low temperature measurements came from the De Lucia laboratory [Willey *et al.* (1988)<sup>3</sup> and (1989),<sup>4</sup> and Beaky *et al.*<sup>20</sup>],

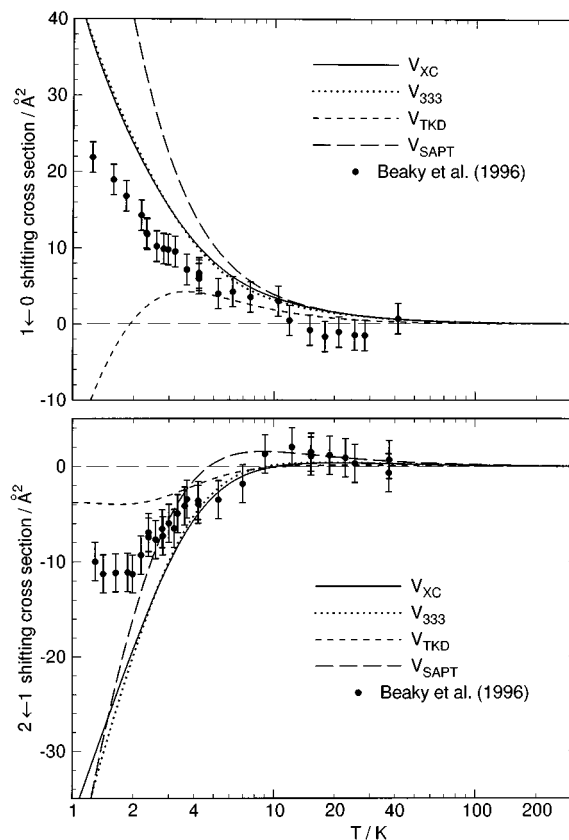


FIG. 10. For the thermal  $j=1\leftarrow 0$  and  $j=2\leftarrow 1$  line shifting cross sections of He-CO, as in Fig. 9.

while the high temperature values are those of Nerf and Sonnenberg<sup>1</sup> and of Nerf.<sup>42</sup> While they show some preference for the predictions yielded by the XC(fit) and  $V_{333}$  potentials, the high temperature broadening cross sections only marginally discriminate among the various potentials. However, the situation is markedly different for the low temperature broadening and shifting cross sections, for which none of the predictions really agree with experiment. In particular, while the TKD predictions of the  $1\leftarrow 0$  broadening cross sections seem in reasonable accord with experiment in the range 1.2–4.2 K, the discrepancies at higher temperatures and for the other three properties suggest that this agreement is fortuitous. At the same time, both sets of pressure shifting cross sections show some preference for the behavior predicted using the XC and  $V_{333}$  potentials, but the residual discrepancies are well beyond the estimated experimental uncertainties.

## IV. DISCUSSION AND CONCLUSIONS

The above results confirm the paradox raised by Chuaqui *et al.*<sup>8</sup> based on calculations using a preliminary version of their  $V_{333}$  potential: the potentials which accurately reproduce the discrete infrared data disagree strongly with the very low temperature line broadening and shifting measurements, in spite of the fact that they are expected to depend on the same region of the potential energy surface. We can en-



vision four possible sources for this discrepancy: (i) inadequacy of the potential energy surface, (ii) problems with the scattering calculations, (iii) deficiencies in the kinetic theory used to relate the scattering cross sections to the bulk line shift and linewidth observables, and (iv) problems with the experiment.

In view of their singular ability to accurately represent the discrete Van der Waals spectra, the XC(fit) and  $V_{333}$  potential energy surfaces are certainly by far the most accurate in the well region, and the results summarized in Table I and in Figs. 2 and 3 suggest that the XC(fit) function is the most accurate overall potential so far reported for this system. For the temperature range from 1 to 4 K, it is this well region on which the line broadening and shifting cross sections *must* be most strongly dependent. The likelihood of finding significant error in the empirical spectroscopic potentials in this region is extremely small, and the good qualitative agreement of their predictions with those yielded by the *ab initio* SAPT surface provides independent confirmation of their reliability. Thus, the present study seems to firmly rule out the potential energy surface being a significant source of error.

The second possible source of error seem equally remote. We believe that the *S*-matrix scattering calculations and the thermal averaging of the resulting cross sections are fully converged and essentially exact. An independent check of this is provided by the accurate agreement between our predictions for the TKD potential and those obtained by Green.<sup>5,6</sup> Thus, we appear to be left with two possibilities: either the error estimates for the very low temperature measurements are overly optimistic, or the theory used to calculate line broadening and shifting cross sections breaks down in this region. The first of these possibilities is addressed in Ref. 20, while one aspect of the second is discussed briefly below.

One assumption invoked in the kinetic theory relating the bulk line shape properties to the individual collision events is the impact approximation, which assumes that only completed collisions contribute to the line broadening and shifting cross sections.<sup>18,19</sup> At the milli-Torr pressures of the experimental measurements, simple kinetic theory arguments indicate that for a plausible assumed collision diameter of 4 Å, the average time between collisions for temperatures in the range 1–4 K would be between 2.5 and 5.0  $\mu$ s. On the other hand, the results of Chuaqui<sup>43</sup> show that the longest-lived resonance states of this species have lifetimes of  $\sim$ 100 ps, while at a collision energy of 1 K the duration of a flyby collision would be only  $\sim$ 10 ps. Thus, it appears that under the conditions of the low temperature experiments the time between collisions is 4–5 orders of magnitude larger than the duration of a collision, so the impact approximation would seem to be valid.

In conclusion therefore, we appear to be left with the possibility that the estimated experimental uncertainties are too small, or that some other aspect of the line shape theory<sup>18,19</sup> breaks down at the very low temperatures associated with the De Lucia group's measurements. However, the

source of the linebroadening and shifting discrepancies and a means of correcting them are not yet known.

## ACKNOWLEDGMENTS

We gratefully acknowledge helpful discussions with Mr. M. M. Beaky and Professors F. C. De Lucia, F. R. W. McCourt, W.-K. Liu, and W. J. Meath, and are pleased to thank Professor M. Faubel for providing us with a copy of the thesis of W. Dilling. This paper is dedicated to the memory of the late Sheldon Green, whose skill, generosity and insight so marvellously graced the field of chemical physics for the past 26 years.

- <sup>1</sup>R. B. Nerf and U. A. Sonnenberg, *J. Mol. Spectrosc.* **58**, 474 (1975).
- <sup>2</sup>J. Messer and F. C. De Lucia, *Phys. Rev. Lett.* **53**, 2555 (1984).
- <sup>3</sup>D. R. Willey, R. L. Crownover, D. N. Bittner, and F. C. De Lucia, *J. Chem. Phys.* **89**, 1923 (1988).
- <sup>4</sup>D. R. Willey, T. M. Goyette, W. L. Ebenstein, D. N. Bittner, and F. C. De Lucia, *J. Chem. Phys.* **91**, 122 (1989).
- <sup>5</sup>S. Green and L. D. Thomas, *J. Chem. Phys.* **73**, 5391 (1980).
- <sup>6</sup>S. Green, *J. Chem. Phys.* **82**, 4548 (1985).
- <sup>7</sup>A. Palma and S. Green, *J. Chem. Phys.* **85**, 1333 (1986).
- <sup>8</sup>C. E. Chuaqui, R. J. Le Roy, and A. R. W. McKellar, *J. Chem. Phys.* **101**, 39 (1994).
- <sup>9</sup>L. D. Thomas, W. P. Kraemer, and G. H. F. Dierksen, *Chem. Phys.* **51**, 131 (1980).
- <sup>10</sup>R. J. Le Roy and J. S. Carley, *Adv. Chem. Phys.* **42**, 353 (1980).
- <sup>11</sup>J. M. Hutson, *Adv. Mol. Vibrations Collision Dynam.* **1A**, 1 (1991).
- <sup>12</sup>J. M. Hutson, in *Dynamics of Polyatomic Van der Waals Complexes*, edited by N. Halberstadt and K. C. Janda (Plenum, New York, 1990).
- <sup>13</sup>Z. Bačić and J. C. Light, *Annu. Rev. Phys. Chem.* **40**, 469 (1989).
- <sup>14</sup>G. Danby, *J. Phys. B: At. Mol. Phys.* **16**, 3393 (1983).
- <sup>15</sup>J. Tennyson, *Comp. Phys. Rep.* **4**, 1 (1986).
- <sup>16</sup>J. Tennyson and S. Miller, *Comp. Phys. Commun.* **55**, 149 (1989).
- <sup>17</sup>T. Slee and R. J. Le Roy, *J. Chem. Phys.* **99**, 360 (1993).
- <sup>18</sup>S. Green, in *Status and Future Developments in Transport Properties*, edited by W. A. Wakeham, (Kluwer Academic, Dordrecht, 1992), p. 257.
- <sup>19</sup>R. Shafer and R. G. Gordon, *J. Chem. Phys.* **58**, 5422 (1973).
- <sup>20</sup>M. M. Beaky, T. M. Goyette, and F. C. De Lucia, preceding paper, *J. Chem. Phys.* **105**, 3994 (1996).
- <sup>21</sup>S. Green and P. Thaddeus, *Astrophys. J.* **205**, 766 (1976).
- <sup>22</sup>W. Dilling, *Doktoral dissertation*, Georg-August-Universität, Göttingen, 1985.
- <sup>23</sup>F. A. Gianturco, N. Sanna, and S. Serna-Molinera, *Mol. Phys.* **81**, 421 (1994).
- <sup>24</sup>R. J. Le Roy, C. Bissonnette, T. H. Wu, A. K. Dham, and W. J. Meath, *Faraday Discuss. Chem. Soc.* **97**, 81 (1994).
- <sup>25</sup>G. C. Maitland, M. Rigby, E. B. Smith, and W. A. Wakeham, *Intermolecular Forces—Their Origin and Determination* (Oxford University Press, Oxford, 1981).
- <sup>26</sup>A. D. Buckingham, P. W. Fowler, and J. M. Hutson, *Chem. Rev.* **88**, 963 (1988).
- <sup>27</sup>R. C. Cohen and R. J. Saykally, *J. Phys. Chem.* **90**, 1024 (1992).
- <sup>28</sup>J. M. Hutson, *Annu. Rev. Phys. Chem.* **41**, 123 (1990).
- <sup>29</sup>R. J. Saykally, *Science* **259**, 1570 (1993).
- <sup>30</sup>B. Kukawska-Tarnawska, G. Chalasinski, and K. Olszewski, *J. Chem. Phys.* **101**, 4964 (1994).
- <sup>31</sup>F.-M. Tao, S. Drucker, R. C. Cohen, and W. Klemperer, *J. Chem. Phys.* **101**, 8680 (1994).
- <sup>32</sup>R. Moszynski, T. Korona, P. E. S. Wormer, and A. van der Avoird, *J. Chem. Phys.* **103**, 321 (1995).
- <sup>33</sup>A. K. Dham and W. J. Meath, *Mol. Phys.* **88**, 339 (1996).
- <sup>34</sup>K. H. Kohl, *Doktoral dissertation*, Universität Göttingen, Göttingen, 1982.
- <sup>35</sup>M. Faubel, K. H. Kohl, and J. P. Toennies, *J. Chem. Phys.* **73**, 2506 (1980).
- <sup>36</sup>J. M. Hutson and S. Green, MOLSCAT computer code, version 14 (1994), distributed by Collaborative Computational Project No. 6 of the Science and Engineering Research Council, U.K., 1994.
- <sup>37</sup>D. E. Manolopoulos, *J. Chem. Phys.* **85**, 6425 (1986).

<sup>38</sup>T. D. Varberg and K. M. Evenson, *Astrophys. J.* **385**, 763 (1992).

<sup>39</sup>This result differs markedly with the calculations presented by Gianturco *et al.* (Ref. 23) which show a dramatic loss of structure with increasing  $j$  (*initial*). The source of this discrepancy is not understood.

<sup>40</sup>M. Faubel, informal comments at the NATO conference of the “Status

and Future Developments in Transport Properties” (1992).

<sup>41</sup>M. Thachuk and F. R. W. McCourt, *J. Chem. Phys.* **94**, 4699 (1991).

<sup>42</sup>R. B. Nerf (private communication to S. Green, quoted in Ref. 5).

<sup>43</sup>C. E. Chuaqui, Ph.D. thesis, Department of Chemistry, University of Waterloo, 1994.